Half–magnetization plateau stabilized by structural distortion in the antiferromagnetic Heisenberg model on a pyrochlore lattice

Karlo Penc,[1] Nic Shannon,[2,3] and Hiroyuki Shiba[4]

[1] *Research Institute for Theoretical Solid State Physics and Optics, H-1525 Budapest, P.O.B. 49, Hungary*
[2] *Department of Advanced Materials Science, Graduate School of Frontier Sciences, University of Tokyo, 5–1–5, Kashiwahnoha, Kashiwa, Chiba 277–8851, Japan*
[3] *CREST, Japan Science and Technology Agency, Kawaguchi 332-0012, Japan*
[4] *The Institute of Pure and Applied Physics, 6-9-6 Shinbashi, Tokyo 105-0004*

(Dated: February 2, 2008)

Magnetization plateaus, visible as anomalies in magnetic susceptibility at low temperatures, are one of the hallmarks of frustrated magnetism. We show how an extremely robust half–magnetization plateau can arise from coupling between spin and lattice degrees of freedom in a pyrochlore antiferromagnet, and develop a detailed symmetry of analysis of the simplest possible scenario for such a plateau state. The application of this theory to the spinel oxides $CdCr_2O_4$ and $HgCr_2O_4$, where a robust half magnetization plateau has been observed, is discussed.

PACS numbers: 75.10.-b, 75.10.Hk 75.80.+q

Spinels, with chemical formula AB_2O_4, are ubiquitous among magnetic oxides. Notable examples of such materials include Fe_3O_4, a system exhibiting frustrated charge order and ferrimagnetism [1], the d–electron heavy fermion compound LiV_2O_4 [2], and the frustrated $S = 3/2$ antiferromagnet $ZnCr_2O_4$ [3]. In all of these compounds, the B–site ion is magnetic, and much of the beautiful strangeness seen in the behaviour of these compounds can be traced back to the fact that the B–site ions form an acutely frustrated *pyrochlore* lattice, built entirely of corner–sharing tetrahedra (Fig. 1).

The geometric frustration of the pyrochlore lattice is so great that both the classical ($S = \infty$) and quantum ($S = 1/2$) antiferromagnetic (AF) Heisenberg models are believed to remain magnetically disordered down to $T = 0$ [4, 5]. In real spinel oxides, however, the ground state degeneracy associated with the frustrated lattice geometry is usually lifted by a distortion of the lattice. $ZnCr_2O_4$, for example, undergoes a transition from a paramagnet with cubic symmetry to a Néel ordered phase with tetragonal symmetry at $T = 12K$.

Another, more progressive, means of reducing the ground state degeneracy of a frustrated AF is to apply a magnetic field. Fields h greatly in excess of the exchange coupling J between spins will remove magnetic frustration altogether and cause the system to become ferromagnetic. At intermediate fields $h \sim J$, frustrated AF's frequently undergo a succession of phase transitions, with associated anomalies in their magnetic susceptibility. Where one particular state remains stable for a finite range of fields, a plateau is seen in the magnetization curve $M(h)$. Magnetization plateaus have been predicted to occur in both triangular lattice and Kagome AF's [6, 7, 8, 9]. In pure spin models, such plateaus occur as an "order from disorder effect" where quantum or thermal fluctuations select one of many possible classical ground states[10]. For this reason they are usually very fragile, and relatively difficult to observe in experiment.

In this letter we consider the interplay between magnetic field, spin, and lattice degrees of freedom in a Heisenberg antiferromagnet on the pyrochlore lattice. Our main result is that the coupling of applied magnetic field to lattice distortion provides an extremely efficient mechanism for stabilizing a robust half–magnetization plateau, with exactly three up spins and one down spin in each tetrahedral sub–unit of the lattice. In principle, many such states may arise; we develop a detailed symmetry analysis of the simplest case, in which all of the tetrahedra which go to make up the lattice distort in the same manner.

Our analysis is of direct relevance to spinel oxides such as $ZnCr_2O_4$, where the A–site ion is non–magnetic, and the octahedrally co–ordinated B–site ion has an exactly half–filled t_{2g} shell of d–electrons, giving rise to a spin $S = 3/2$ moment. And, indeed, just such a plateau has been observed in recent high field magnetization measurements on the closely related Cr spinels $CdCr_2O_4$ and

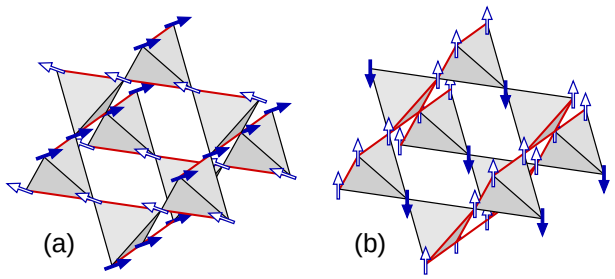

FIG. 1: A section of the pyrochlore lattice, showing its two–sublattice tetrahedral structure. At zero–magnetization, tetragonal lattice distortion favors the spin configurations of the type shown in (a), while at half–magnetization trigonal lattice distortion favors the configuration (b). AF bonds are marked with black and FM bonds with red lines.

$HgCr_2O_4$ [11].

We take as a starting point the Hamiltonian

$$\mathcal{H} = \sum_{\langle i,j \rangle} \left[J(1-\alpha_1 \rho_{i,j}) \mathbf{S}_i \mathbf{S}_j + \frac{K}{2} \rho_{i,j}^2 \right] - \mathbf{h} \sum_i \mathbf{S}_i \ , \quad (1)$$

where the summation $\langle i,j \rangle$ runs over the nearest neighbor bonds of a pyrochlore lattice and $\rho_{i,j}$ is the change in distance between neighboring spins $\mathbf{S}_i$ and $\mathbf{S}_j$, relative to the equilibrium lattice constant. We assume the existence of a linear regime in which exchange interactions and elastic energies depend only on the distance between lattice sites. It is convenient to introduce a single dimensionless parameter $b = J\alpha^2/K$ to measure the strength of the spin–lattice coupling. As written, the antiferromagnetic exchange interaction J, elastic constant K and a spin–lattice coupling α, are all taken to be positive.

The pyrochlore is a bipartite network of corner sharing tetrahedra. This means that, if we neglect coupling to the lattice, we can write the energy per spin as

$$\mathcal{H} = 4J \sum_{\text{tetr.}} \left(\mathbf{M} - \frac{\mathbf{h}}{8J} \right)^2 - \frac{h^2}{16J} + \text{const.} \ , \quad (2)$$

where the sum runs over all the tetrahedra and $\mathbf{M} = (\mathbf{S}_1 + \mathbf{S}_2 + \mathbf{S}_3 + \mathbf{S}_4)/4$ is the magnetization per site. Clearly, the energy can be minimized by ensuring $\mathbf{M} = \mathbf{h}/8$ in each tetrahedron. However this local constraint does not select any one ground state, but rather a vast manifold of states. If we consider classical spins, one angular variable remains undetermined per tetrahedron, and the magnetization is linear in h right up the saturation field of $h = 8J$.

Coupling to the lattice provides a very efficient mechanism for lifting this degeneracy. Since bond energies vary linearly with $\rho_{i,j}$, while elastic energies increase as $\rho_{i,j}^2$, at any given value of magnetic field the system can always gain energy by ordering the spins and distorting the lattice. In this sense the Hamiltonian (1) can be thought of as a three dimensional generalization of the spin–Peierls problem. The system gains the most energy from distorting bonds for which $\mathbf{S}_i \mathbf{S}_j$ takes on its extremal values. For this reason, coupling to the lattice tends to favor collinear spin configurations and, for quantum spins, bond singlets (see e.g. [12]). Our goal is to understand which states emerge from this competition between applied field and frustrated AF interactions, and for what range of fields they are stable.

For the sake of simplicity, and in the spirit of earlier work [13, 14], we shall restrict our analysis to uniform spin and lattice order with crystal momentum $q = 0$. It is instructive to further simplify the problem by treating the spins as classical vectors, in which case we can safely neglect all states which are odd under the inversion $\mathcal{I}_T$ which exchanges the two tetrahedron sublattices. Both of these approximations can be relaxed at will.

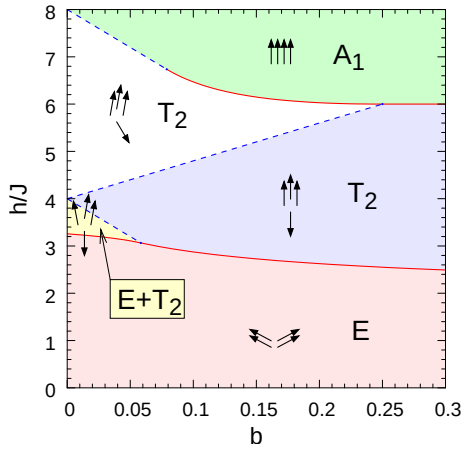

FIG. 2: Phase diagram as a function of magnetic field h and dimensionless coupling constant b. Solid lines denote first and dashed lines second order transitions. Spin configurations and irrep of the order parameter in each phase is also shown.

Under these assumptions, the system must have four sublattice order, and we can find the ground state of Eq. (1) by a straightforward minimization of energy with respect to bond length. This is equivalent to solving a Heisenberg model with biquadratic–bilinear terms[15] :

$$\mathcal{H} = \sum_{\langle i,j \rangle} J \left[\mathbf{S}_i \mathbf{S}_j - b(\mathbf{S}_i \mathbf{S}_j)^2 \right] - \mathbf{h} \sum_i \mathbf{S}_i \ . \quad (3)$$

Our results are summarized in the phase diagram Fig. 2, with the corresponding magnetization curves shown in Fig. 3. For small h, the lattice has overall tetragonal symmetry, with tetrahedra distorted so as to have two long ferromagnetic (FM) and four short canted AF bonds. This is broadly compatible with the experimentally observed ground state of $ZnCr_2O_4$ [3]. In this regime the magnetization of the system remains linear, but with reduced slope $M \approx h/(8J(1+2b))$.

For $h \approx 3J$, and $b \gtrsim 0.05$ the system makes a first order transition into state with exactly 3 up and 1 down spins per tetrahedron, i.e. $M \equiv S/2$, regardless of h. In this half–magnetization "plateau" phase, each tetrahedron has three long FM and three short AF bonds, giving rise to an overall trigonal lattice distortion. For any finite value of b the plateau is extremely broad. Its width shrinks linearly as $b \to 0$; for $h/J \leq 4 - 16b$ we find a transition into a coplanar 2:1:1 canted state with mixed E and T_2 symmetry, and for $h/J = 4 + 8b$ a transition into a coplanar 3:1 canted phase with trigonal symmetry for $h/J = 4 + 8b$. Both transitions are of second order.

Finally, for $8J > h > 6J$, there is a transition into a fully saturated FM in which the lattice regains overall cubic symmetry. In the absence of longer range exchange interactions, the two lowest lying spin wave branches of the FM phase are local in character and dispersionless. For $b < 3/38$, the transition from the 3:1 canted phase

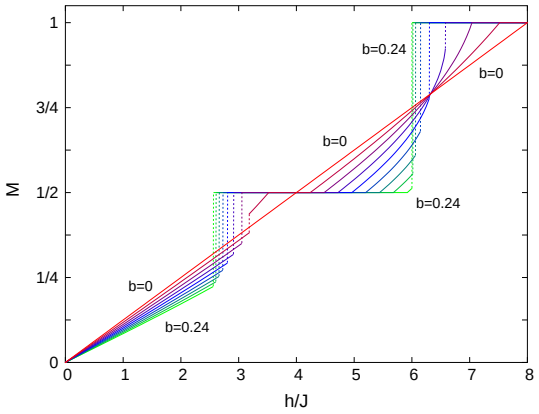

FIG. 3: Magnetization as a function of magnetic field for $b = 0$ (straight line) to $b = 0.24$ (robust plateau) in steps of 0.03.

into the FM is of second order, and occurs on the line $h/J = 8 - 16b$. For $b > 3/38$ the transition becomes first order, and for $b > 1/4$ it is energetically favorable to make a transition directly from the collinear plateau phase into the FM.

In order to understand *why* these particular phases are stable, we now turn to the symmetry analysis. For classical spins, coupled to uniform lattice distortion, we need only consider the symmetries $\mathcal{T}_d$ of a single tetrahedron [16]. The bond variables $\rho_{i,j}$, which describe changes in the length of the six edges of the tetrahedron, transform according to the A_1, E, and T_2 irreducible representations (irreps) of $\mathcal{T}_d$:

$$\begin{pmatrix} \rho_{\mathsf{A}_1} \\ \rho_{\mathsf{E},1} \\ \rho_{\mathsf{E},2} \\ \rho_{\mathsf{T}_2,1} \\ \rho_{\mathsf{T}_2,2} \\ \rho_{\mathsf{T}_2,3} \end{pmatrix} = \begin{pmatrix} \frac{1}{\sqrt{6}} & \frac{1}{\sqrt{6}} & \frac{1}{\sqrt{6}} & \frac{1}{\sqrt{6}} & \frac{1}{\sqrt{6}} & \frac{1}{\sqrt{6}} \\ \frac{1}{\sqrt{3}} & \frac{-1}{2\sqrt{3}} & \frac{-1}{2\sqrt{3}} & \frac{-1}{2\sqrt{3}} & \frac{-1}{2\sqrt{3}} & \frac{1}{\sqrt{3}} \\ 0 & \frac{1}{2} & -\frac{1}{2} & -\frac{1}{2} & \frac{1}{2} & 0 \\ 0 & 0 & \frac{-1}{\sqrt{2}} & \frac{1}{\sqrt{2}} & 0 & 0 \\ 0 & \frac{-1}{\sqrt{2}} & 0 & 0 & \frac{1}{\sqrt{2}} & 0 \\ \frac{-1}{\sqrt{2}} & 0 & 0 & 0 & 0 & \frac{1}{\sqrt{2}} \end{pmatrix} \begin{pmatrix} \rho_{1,2} \\ \rho_{1,3} \\ \rho_{1,4} \\ \rho_{2,3} \\ \rho_{2,4} \\ \rho_{3,4} \end{pmatrix} \tag{4}$$

In the $\boldsymbol{\rho}_{\mathsf{E}} = \{\rho_{\mathsf{E},1}, \rho_{\mathsf{E},2}\}$ irrep (which includes tetragonal distortions of the lattice), opposing pairs of bonds deform with the same sense. In the $\boldsymbol{\rho}_{\mathsf{T}_2} = \{\rho_{\mathsf{T}_2,1}, \rho_{\mathsf{T}_2,2}, \rho_{\mathsf{T}_2,3}\}$ irrep (which includes trigonal distortions), opposing pairs of bonds deform with the opposite sense. Exactly analogous representations for spins can be obtained by substituting with $\mathbf{S}_i\mathbf{S}_j$ for $\rho_{i,j}$ and Λ_{A_1} for ρ_{A_1}, etc.

In terms of these variables, the Hamiltonian for a single tetrahedron embedded in the lattice is given by

$$\begin{aligned} \mathcal{H} &= 2\sqrt{6}J\Lambda_{\mathsf{A}} - 2\alpha J\left(\Lambda_{\mathsf{A}}\rho_{\mathsf{A}} + \boldsymbol{\Lambda}_{\mathsf{E}}\boldsymbol{\rho}_{\mathsf{E}} + \boldsymbol{\Lambda}_{\mathsf{T}_2}\boldsymbol{\rho}_{\mathsf{T}_2}\right) \\ &\quad + K\left(\rho_{\mathsf{A}}^2 + \rho_{\mathsf{E}}^2 + \rho_{\mathsf{T}_2}^2\right) - 4\mathbf{h}\mathbf{M}\,, \end{aligned} \tag{5}$$

where $\boldsymbol{\Lambda}_{\mathsf{R}}\boldsymbol{\rho}_{\mathsf{R}}$ and $\rho_{\mathsf{R}}^2 = \boldsymbol{\rho}_{\mathsf{R}}\boldsymbol{\rho}_{\mathsf{R}}$ are second order invariants of the $\mathsf{R} = \mathsf{A}_1, \mathsf{E}$, and T_2 irreps. An analysis of Eq. (5) in the absence of magnetic field was given in Refs. [13] and [14]. In all of the cases considered by these authors, only the E irrep is relevant. However, once a magnetic field is applied, both the A_1 and T_2 irreps have an important role to play. For classical spins, Eq. (5) reduces to

$$E_0 = 2J\left(\sqrt{6}\Lambda_{\mathsf{A}_1} - b_{\mathsf{A}_1}\Lambda_{\mathsf{A}_1}^2 - b_{\mathsf{E}}\Lambda_{\mathsf{E}}^2 - b_{\mathsf{T}_2}\Lambda_{\mathsf{T}_2}^2\right) - 4\mathbf{h}\mathbf{M}\,. \tag{6}$$

For pure nearest neighbour interaction [c.f. Eq. (1)] $b_{\mathsf{A}_1} = b_{\mathsf{E}} = b_{\mathsf{T}_2} = b$. In general, however, these parameters need not be equal.

Using the fact that $\Lambda_{\mathsf{A}_1} = 8(M^2 - 1/4)/\sqrt{6}$, we see that the lowest energy configuration at a given magnetization is that for which $b_{\mathsf{E}}\Lambda_{\mathsf{E}}^2 + b_{\mathsf{T}_2}\Lambda_{\mathsf{T}_2}^2$ takes on its maximal value. The surface of maximal values of these second order invariants is shown in Fig. 4. The limiting cases $\Lambda_{\mathsf{T}_2} \to 0$ or $\Lambda_{\mathsf{E}} \to 0$ have a simple analytic form

$$\max_{\Lambda_{\mathsf{T}_2}^2=0} \Lambda_{\mathsf{E}_2}^2 \;=\; 16(1-M^2)^2/3\,, \tag{7}$$

$$\max_{\Lambda_{\mathsf{E}}^2=0} \Lambda_{\mathsf{T}_2}^2 \;=\; \begin{cases} \frac{32}{3}\left(1-M^2\right)^2\,, & \text{if } 1/2 \le M \le 1\,; \\ \frac{32}{3}M^2(1+M)^2\,, & \text{if } 0 \le M \le 1/2\,. \end{cases} \tag{8}$$

and the stability of the half–magnetization plateau originates in the sharp cusp in the maximal value of Λ_{T}^2 as a function of M. Provided that $b_{\mathsf{E}} < 2b_{\mathsf{T}_2}$, this singular point (which corresponds to the trigonal lattice distortion shown in Fig. 1b), minimizes the energy for a finite range of values of magnetic field, and the phase diagram is qualitatively that of Fig. 2. Conversely, for values of $b_{\mathsf{E}} > 2b_{\mathsf{T}_2}$, T_2 order is not realized for any value of h.

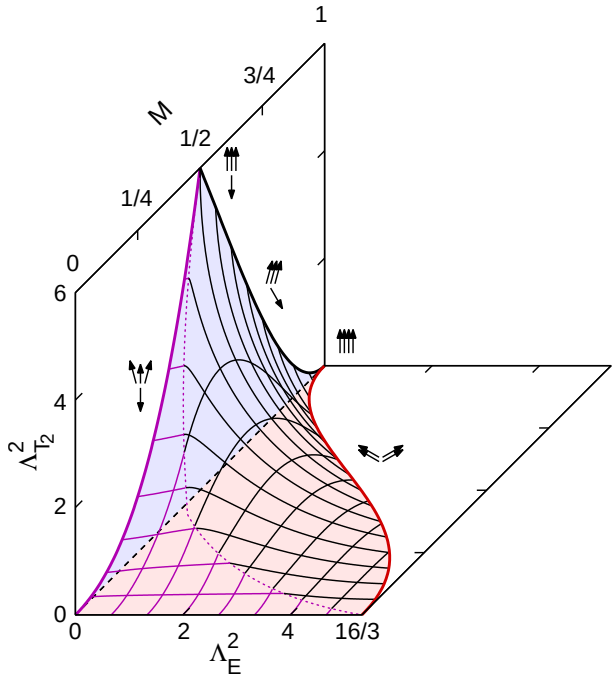

FIG. 4: Maximal values of the second order invariants Λ_{E}^2 and $\Lambda_{\mathsf{T}_2}^2$ for classical spins as a function of the magnetization per site M. A ridge (dashed line) divides three dimensional from coplanar spin configurations. Spin ordering patterns are shown for the symmetrical cases of $\Lambda_{\mathsf{E}}^2 = 0$ and $\Lambda_{\mathsf{T}_2}^2 = 0$.

As the magnetization of the system increases, so will the average bond length, and for classical spins coupled to a uniform lattice distortion, the volume of the unit cell is a monotonically increasing function of applied field

$$\frac{\delta V}{V} = \sqrt{\frac{3}{2}}\rho_{\mathsf{A}_1} + \frac{1}{2}\rho^2_{\mathsf{A}_1} - \frac{7}{4}\rho^2_{\mathsf{E}} - \frac{3}{4}\rho^2_{\mathsf{T}_2} \, . \qquad (9)$$

From this expression we learn that: (i) as $\rho_{\mathsf{A}_1} \propto \Lambda_{\mathsf{A}_1}$, the jumps in magnetization will have their counterpart in volume change; (ii) the application of hydrostatic pressure will soften the E mode relative to the T_2 mode, thus extending the region of the tetragonal phase.

The scenario which we have presented is the simplest under which lattice distortion can stabilize a magnetization plateau in a spinel oxide. Needless to say, the situation in a real spinel oxide may be much more complex than that described above. Naive estimates suggest that there are of order $1.3^{N/2}$ collinear states with 3 up and 1 down spins in each tetrahedron, where N is the number of spins in the lattice. In principle, any of these may couple to phonon modes. Arbitrarily complex exchange interactions, competing with arbitrarily complex elastic energies, may give rise to an arbitrarily complex plateau state — or none at all. None the less, our model captures the essential features of the high field magnetization of $CdCr_2O_4$ and $HgCr_2O_4$ [11]. For these Cr spinels t_{2g} shell is full and the e_g shell empty, so we may safely neglect the effects of orbital degeneracy [17]. The theory may also be applicable to $ZnCr_2O_4$, although the high value of J in this compound makes verification difficult.

Chromium spinels exist as chalcogenides as well as oxides[18]. The chalcogenides have weaker and predominately FM interactions, and are therefore less likely *a priori* to exhibit a half–magnetization plateau. However the competition between FM and AF interactions is already present in oxide materials. We have examined the role of next–nearest neighbour exchange J_2 within spin wave theory, the minimization of the energy of small clusters, and an extension of the symmetry analysis presented above. For AF J_2, $b_{\mathsf{T}_2} > b_{\mathsf{E}}$, and the stability of the trigonal half–magnetization plateau phase is enhanced. FM J_2, on the other hand, drives the system towards lattice distortions (and associated plateau states) at finite q. It is also worth noting that the strength and sign of exchange interactions in oxides and chalcogenides can be very sensitive to bond angle. As written, the Eq. (1) does not allow for the rotation of neighboring tetrahedra at fixed bond length. Such modes will be important at finite q, and may lead to a magnetostriction (i.e. decrease in the volume of the unit cell at in applied field). The necessary extension of our theory to treat these cases is in principle possible, but lies beyond the scope of the present letter.

We conclude with a few comments on the role of fluctuations. In constructing a theory of a half–magnetization plateau stabilized by lattice distortion we have assumed static spin order. Since both quantum and thermal fluctuations in frustrated magnets favour collinear spin configurations [19], these will further contribute to the stability of the magnetization plateau. If consider Eq. (3) as an effective hamiltonian, the coefficient b will have contributions fluctuation effects as well as lattice distortion [20]. It may also have contributions of a purely electronic origin [21]. However, we have performed monte carlo simulations of Eq. (1) for classical spins in the absence of coupling to the lattice, and these suggest that any plateau stabilized by "order from disorder" effects alone will be at least as fragile as that seen in the Kagome lattice [9]. The remarkable width of the half–magnetization plateaus observed in $CdCr_2O_4$ and $HgCr_2O_4$ — which extend over many tesla — leads us to the conclusion that lattice distortion plays a crucial role in these systems.

We are pleased to acknowledge helpful discussions with S. W. Cheong, P. Fazekas, M. Hagiwara, H. Katori, M. Matsuda, H. Takagi, O. Tchernyshyov, H. Tsunetsugu, H. Ueda, and K. Ueda. We are particularly grateful to the authors of [11] for supplying us with their data prior to publication. We thank the support of the Hungarian OTKA T038162 and JSPS–HAS joint project.

[1] P. W. Anderson, Phys. Rev. **102**, 1008 (1956).
[2] C. Urano et al., Phys Rev Lett **85**, 1052 (2000).
[3] S. –H. Lee et al, Nature **418**, 856 (2002); S. –H. Lee et al., Phys. Rev. Lett. **84**, 3718 (2000).
[4] R. Moessner and J. Chalker, Phys. Rev. B **58**, 12049 (1998).
[5] B. Canals and C. Lacroix, Phys. Rev B **61**, 1149 (2000).
[6] S. Miyashita, J. Phys. Soc. Jpn. **55**, 3605 (1986).
[7] A. Chubukov and D. I. Golosov, J. Phys Condens. Mater **3**, 69 (1989).
[8] T. Momoi et al, Phys. Rev. B **59**, 9491 (1999).
[9] M. E. Zhitomirsky, Phys. Rev. Lett. **88**, 057204 (2002).
[10] M. E. Zhitomirsky et al., Phys. Rev. Lett. **85**, 3269 (2000).
[11] H. Ueda, et al., unpublished.
[12] F. Becca and F. Mila, Phys. Rev. Lett. **89**, 037204 (2002).
[13] Y. Yamashita and K. Ueda, Phys. Rev. Lett. **85**, 4960 (2000).
[14] O. Tchernyshyov, et al. Phys. Rev. Lett. **88**, 067203 (2002); Phys. Rev B **66**, 064403 (2002).
[15] C. Kittel, Phys. Rev. **120**, 335 (1960).
[16] Formally, the point group of the pyrochlore lattice is $\mathcal{O}_h \equiv \mathcal{T}_d \otimes \{1, \mathcal{I}_T\}$; here by construction we work only with states even in $\mathcal{I}_T$.
[17] H. Tsunetsugu and Y. Motome, Phys. Rev. B **68**, 060405 (2003).
[18] P. Baltzer et al., Phys. Rev. **151**, 367 (1966).
[19] C. Henley, Phys. Rev. Lett. **62**, 2056 (1989).
[20] H. Shiba et al., J. Phys. Soc. Jpn. **69**, 1484 (2000).
[21] J. C. M. Henning et al., Phys. Rev. B **7**, 1825 (1973).